Geophysical Research Letters

RESEARCH LETTER
10.1029/2024GL110485

Influence of SST-Precipitation Relationship Over the Equatorial Western Pacific on Simulation of the Madden-Julian Oscillation

Guiwan Chen[1], Jian Ling[1,2], Ziniu Xiao[1,3], Chongyin Li[3], and Chidong Zhang[4]

[1]Key Laboratory of Earth System Numerical Modeling and Application, Institute of Atmospheric Physics, Beijing, China, [2]Collaborative Innovation Center on Forecast and Evaluation of Meteorological Disasters, Nanjing University of Information Science and Technology, Nanjing, China, [3]State Key Laboratory of Numerical Modelling for Atmospheric Sciences and Geophysical Fluid Dynamics, Institute of Atmospheric Physics, Beijing, China, [4]NOAA Pacific Marine Environmental Laboratory, Seattle, WA, USA

Key Points:

- Madden-Julian Oscillation (MJO) simulation skills depend on organized large-scale precipitation over the equatorial western Pacific (EWP) reproduced in models
- Models with higher MJO simulation skills exhibit lower sea surface temperature (SST) threshold for convection over the EWP
- Realistically reproducing the relationship between the SST and organized large-scale precipitation is critical to MJO simulations

Supporting Information:

Supporting Information may be found in the online version of this article.

Correspondence to:

J. Ling,
lingjian@lasg.iap.ac.cn

Citation:

Chen, G., Ling, J., Xiao, Z., Li, C., & Zhang, C. (2024). Influence of SST-precipitation relationship over the equatorial western Pacific on simulation of the Madden-Julian Oscillation. *Geophysical Research Letters*, *51*, e2024GL110485. https://doi.org/10.1029/2024GL110485

Received 29 MAY 2024
Accepted 16 OCT 2024

Abstract Capabilities of 43 models of the Coupled Model Intercomparison Project Phase 6 (CMIP6) to simulate the Madden-Julian Oscillation (MJO) were compared in this study. Models with higher MJO simulation skills reproduce organized large-scale convection more frequently over the equatorial western Pacific (EWP), suggesting that MJO simulations are tightly connected to organization of large-scale precipitation over the EWP. MJO simulation skills are not significantly correlated with the mean sea surface temperature (SST) over the EWP, but tightly connected to SST threshold for convection there. The top simulations exhibit lower SST threshold and more realistic SST-precipitation relationship over the EWP, suggesting that convection can be organized more efficiently and intensified more rapidly with the increasing SST in these simulations. Our results emphasize that reproducing the relationship between SST and large-scale precipitation over the EWP is critical to MJO simulations.

Plain Language Summary The Madden-Julian Oscillation (MJO) is one of the most important tropical phenomena that modulate weather and climate systems at the intraseasonal time scales. However, accurately reproducing the MJO in global climate models remains a challenge. The eastward propagation of the MJO convection is usually not well-reproduced in models. Comparing to observations, they tend to underestimate the occurrence frequency of individual MJO events with lower amplitude and shorter propagation range. This study explore whether the MJO simulations in models are linked to the relationship between sea surface temperature (SST) and large-scale precipitation they reproduced. It was found that MJO simulation skills are greatly dependent on the organized large-scale precipitation over the equatorial western Pacific. We further revealed that realistically reproducing the SST-precipitation relationship over this region is critical for simulating the MJO in models.

1. Introduction

The Madden-Julian Oscillation (MJO; Madden & Julian, 1971, 1972) is characterized by eastward propagating large-scale convection systems from the Indian Ocean to the western-central Pacific with speeds of 3–7 m s^{-1} (Zhang & Ling, 2017). Accurately reproducing the eastward propagation of the MJO convection remains a major challenge to global climate models (GCMs; Ahn et al., 2020; Chen, Ling, Zhang, Xiao, & Li, 2022; Hung et al., 2013; Jiang et al., 2015; Ling et al., 2017). GCMs tend to exhibit stationary oscillations of large-scale precipitation (Ahn et al., 2020; Hung et al., 2013; Jiang et al., 2015). They often underestimate the frequency of individual MJO events and exaggerate the barrier effect of the Maritime Continent on MJO propagation (Chen et al., 2020, 2022a; Ling et al., 2017, 2019). The challenges of reproducing the MJO in GCMs are linked to systematic errors in the mean state (Ahn et al., 2020; Chen, Ling, Zhang, Wang, & Li, 2022; Gonzalez & Jiang, 2017; Inness et al., 2003; Ling et al., 2017). Dry biases of low-level moisture over the Indo-Pacific warm pool region, which lead to an underestimation of the meridional moisture gradient, are associated with poor representations of the MJO propagation in GCMs (Ahn et al., 2020; Gonzalez & Jiang, 2017; Ling et al., 2017).

The capability of GCMs in simulating the MJO also depends on the organization of large-scale precipitation. GCMs with more frequent organized large-scale precipitation systems over the Indo-Pacific warm pool exhibit higher MJO simulation skills, owning to their rapid organization of precipitation systems into spatial scales of

thousands of kilometers (Chen et al., 2021). Previous studies have also suggested that a warmer sea surface temperature (SST) over the Indo-Pacific warm pool regions could induce stronger MJO signals in GCMs (Arnold et al., 2013; Inness et al., 2003; Sperber, 2004). Nevertheless, the connection between the large-scale precipitation organization of the MJO and the mean SST in GCMs remains ambiguous. Large-scale convection in the tropics generally occurs more frequently as SST becomes higher (Bjerknes, 1966, 1969), but their relationship is nonlinear. Deep convection generally arises when the SST exceeds 27°C (Gadgil et al., 1984; Graham & Barnett, 1987; Hu et al., 2023; Johnson & Xie, 2010; Leung et al., 2022). The SST threshold for deep convection to occur, however, vary seasonally and regionally. Deep convection intensifies with increasing SST at the range of 27°C–29.5°C. In regions of SST exceeding 29.5°C deep convection is usually weaker (Gadgil et al., 1984; Lau et al., 1997; Sabin et al., 2013; Waliser et al., 1993; Zhang, 1993). It remains unclear whether the capability of GCMs to simulate the MJO rely on the accuracy of reproducing the observed relationship between SST and large-scale precipitation.

In this study, we aim at addressing this question by comparing MJO simulations and SST-precipitation relationships in the outputs from 43 models of the Coupled Model Intercomparison Project Phase 6 (CMIP6). The data sets and methods utilized were introduced in Section 2. The results are described in Section 3, followed by conclusions and discussions in Section 4.

2. Data and Methods

Daily precipitation and monthly SST data covering the period of 1979–2014 from the historical simulations of 43 CMIP6 models (Table S1 in Supporting Information S1) were used in this study. Daily precipitation from the Tropical Rainfall Measuring Mission (TRMM) 3B42 Version 7 (Huffman et al., 2007) and monthly SST from the Optimum Interpolation SST (OISST) Version 2.1 (Huang et al., 2021) from 1998 to 2018 were used for observational validation. These data sets were interpolated into an uniform horizontal resolution of 2.5° in latitude and longitude. This study focuses on the extended boreal winter of October–March during which the eastward propagation of the MJO is most prominent.

Characteristics of individual MJO events can be quantitively obtained using the MJO tracking method proposed by Zhang and Ling (2017). In this study, a combined metric that defined as the mean of four characteristics of the MJO normalized by the TRMM observations is used to qualify the capability of models to simulate the MJO. The MJO characteristics used include the occurrence frequency of MJO, its amplitude in precipitation, its propagation range in longitude, and the ratio of number of MJO events propagating through the Maritime Continent to that entering the Maritime Continent. This MJO skill metric is significantly correlated with individual MJO characteristics, and the MJO skill metrics based on spectral analysis and lead-lag correlation (Figure S1 in Supporting Information S1). The model simulations are group into two catalogs based on their MJO simulation skills: the top 15 simulations with highest MJO simulation skills and the bottom 15 simulations with lowest MJO simulation skills. Comparing to the bottom 15 simulations, the top 15 simulations can reproduce better power spectral signals (Figure S2 in Supporting Information S1) and eastward propagating precipitation envelopes (Figure S3 in Supporting Information S1) of the MJO.

To identify large-scale precipitation that organized on spatial scales of thousands of kilometers, the large-scale precipitation tracking method (Kerns & Chen, 2020) was utilized. The filtered precipitation was obtained by applying a 3-day running mean to the daily precipitation. A two-dimensional Gaussian smoother with a standard deviation of 4 contiguous grid points (5° in latitude and longitude) extending out three standard deviations in each direction was then applied. Rainfall contours of filtered precipitation exceeding 12 mm d^{-1} with a minimum of 4 contiguous grid cells (with diagonal connectivity excluded) are identified as large-scale precipitation object (LPO). The precipitation within the LPO contours and a peripheral zone of one filter standard deviation (5° latitude/longitude) outside of the LPO contours are defined as the LPO precipitation. Precipitation that is not associated with LPOs is defined as Non-LP precipitation. LPO precipitation represents the coherent and organized large-scale precipitation with spatial scales of thousands of kilometers. The area of an LPO defined as the sum of the areas of each of the grid cells that encompass the LPO, and the strength of an LPO is measured by the averaged rainfall within the LPO contour and its peripheral zone.

Composites of precipitation, LPO precipitation and Non-LP precipitation for certain model simulations were calculated by averaging the composited precipitation of each individual simulations. The significance for the differences between the top and bottom simulations was assessed by applying the Students' *t*-test at the 95%

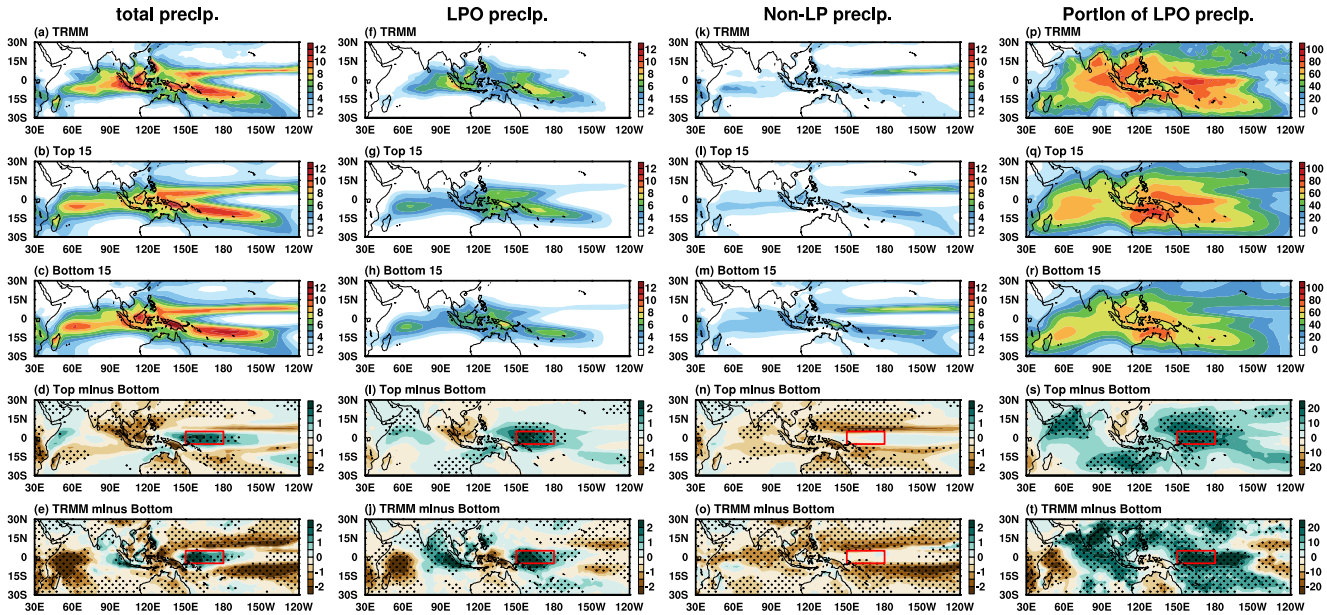

Figure 1. Horizontal distributions of boreal winter mean (a–e) total precipitation (mm d^{-1}), (f–j) large-scale precipitation object (LPO) precipitation (mm d^{-1}), (k–o) Non-LP precipitation (mm d^{-1}), and (p–t) portion of LPO precipitation relative to total precipitation (%) in panels (a, f, k, p) the Tropical Rainfall Measuring Mission (TRMM) observations, (b, g, l, q) the top simulations, (c, h, m, r) the bottom simulations, and differences between (d, i, n, s) the top and bottom simulations, as well as panels (e, j, o, t) the TRMM observations and the bottom simulations. Dotted areas mark the differences are significant at the 95% confidence level. The red rectangle marks the equatorial western Pacific (150°E–180°, 5°S–5°N).

confidence level. An inter-model correlation coefficient higher than 0.3 or lower than −0.3 is treated as significant, under the premise that the 43 model simulations are independent samples.

3. Results

Climatologies of precipitation during boreal winter in the TRMM observations, the top and bottom simulations (Figures 1a–1e) were first compared. The top simulations exhibit significantly more precipitation over the equatorial western Pacific (EWP), and less over the subtropical regions of the Maritime Continent than the bottom simulations (Figure 1d). In general, the simulations exhibit common biases of overestimated precipitation over the western Indian Ocean and the intertropical convergence zone (ITCZ), and underestimated precipitation over the eastern Indian Ocean (Figures 1b–1e).

In the TRMM observations, LPO precipitation primarily concentrates over the Indo-Pacific warm pool region (Figure 1f). The top simulations produce more LPO precipitation over the EWP than the bottom simulations (Figure 1i). But they both tend to overestimate LPO precipitation over the western Indian Ocean, and underestimate it over the eastern Indian Ocean comparing to the TRMM observations (Figures 1g–1j). Non-LP precipitation primarily concentrates over the ITCZ, islands of the Maritime Continent, and western Indian Ocean in the TRMM observations (Figure 1k). The top simulations exhibit significantly less Non-LP precipitation than the bottom simulations, especially over the off-equatorial regions (Figure 1n). The bottom simulations obviously overestimate Non-LP precipitation over the tropical regions comparing to the TRMM observations (Figure 1o). More than 50% of the precipitation over the warm pool was contributed by the LPO precipitation in the TRMM observations (Figure 1p). Comparing to the bottom simulations, the top simulations significantly exhibit larger portion of LPO precipitation relative to total precipitation over majority regions of the warm pool, especially over the EWP (Figure 1s). While the bottom simulations obviously underestimate portion of LPO precipitation than the TRMM observations (Figure 1t). These results imply that the MJO simulation skills are tightly linked to how well the large-scale precipitation is organized in the models.

Possible mechanisms that determine the LPO precipitation over the EWP (150°E–180°, 5°S–5°N), where differences of LPO precipitation between the top and bottom simulations are most evident, will be investigated in the rest of the paper. The probability density functions (PDFs) of daily precipitation over the EWP was firstly

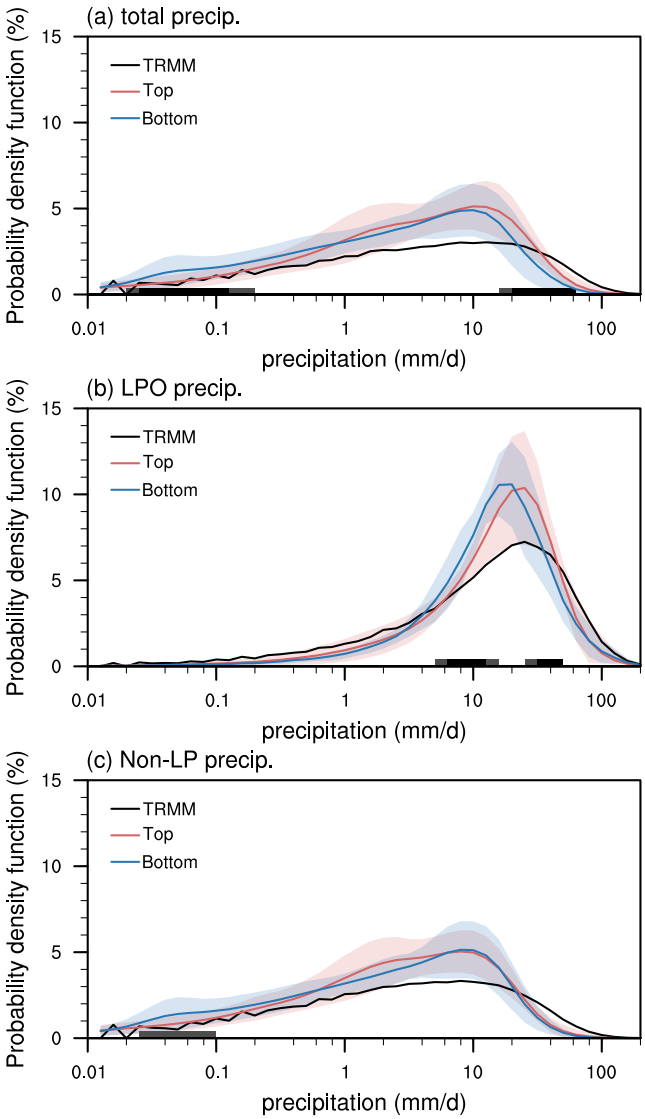

Figure 2. Probability density distributions (%) of panel (a) total precipitation, (b) large-scale precipitation object precipitation, and (c) non-LP precipitation over the equatorial western Pacific (150°E–180°, 5°S–5°N) in the Tropical Rainfall Measuring Mission observations (black curve), the top (red) and bottom simulations (blue). The light red and blue shading indicates inter-model spreads (one standard deviation) of the top and bottom simulations, respectively. The black (gray) bars denote differences between the top and bottom simulations significant at the 95% (90%) confidence level.

evaluated (Figure 2). Days when the precipitation amount is less than 0.01 mm d^{-1} are included in the calculation but not shown. There are 30% of days when the precipitation amount is less than 0.01 mm d^{-1} in the TRMM observations over the EWP, while it is only about 6% in the simulations. The simulations tend to underestimate the probability of heavy rainfall and overestimate the probability of light rainfall, which has been documented as the common bias of GCMs (e.g., Dai, 2006). The PDF of total precipitation in the top simulations is closer to that of the TRMM observations (Figure 2a). The top simulations exhibit significant lower probability of light rainfall (0.02–0.2 mm d^{-1}) and higher probability of heavy rainfall (20–80 mm d^{-1}) than the bottom simulations. The intensity of LPO precipitation is mainly contributed by moderate and heavy rainfall (Figure 2b). For LPO precipitation, the top simulations generally exhibit more heavy rainfall and less moderate rainfall than the bottom simulations, and the PDF of rainfall in the top simulations is more consistent with that of the TRMM observations (Figure 2b). For Non-LP precipitation, there is no significant difference between the top and bottom simulations (Figure 2c), except that the bottom simulations exhibit more light rainfall than the top simulations at the 90% confidence level. This further confirms that the differences in precipitation over the EWP between the top and bottom simulations largely come from the differences in the organized large-scale precipitation.

Significant inter-model correlation between MJO simulation skills and the organized large-scale precipitation over the EWP could depend on the occurrence frequency of LPOs, their spatial scales and strength. If the centroid of an LPO falls into the EWP, it is treated as LPO over the EWP. The probability of the LPO occurrence over the EWP is defined as a ratio of number of days with LPOs over there to the total number of days. It describes how often precipitation can be organized into the large scale over the EWP. It is similar to the concept of organization of deep convective clouds (Biagioli & Tompkins, 2023), except we emphasize the large-scale precipitation organization at the time scales of several days or even longer. There are significant inter-model correlations between MJO simulation skills and the probability of LPO occurrence, averaged area and strength of LPO over the EWP (Figures 3a–3c). These results indicate that models with higher MJO simulation skills reproduce LPOs more frequently over the EWP with larger spatial scales and greater strength. In other word, organizing the precipitation into large-scale over the EWP might be crucial for the MJO simulation (Chen et al., 2021).

There is no significant inter-model correlation between MJO simulation skills and boreal winter mean SST over the EWP (Figure 3d). It suggests that mean SST is not determinant for the organized large-scale precipitation over the EWP. The SST threshold for convection might be more critical. Following Johnson and Xie (2010), the mean precipitation corresponding to SST binned at intervals of 0.1°C was calculated based on monthly precipitation and SST over each grid of the EWP during boreal winter. Then, the minimum SST of 3 consecutive bins with mean precipitation exceeds 3 mm d^{-1} is considered as the SST threshold for convection. As expected, a higher SST threshold for convection in the models generally corresponds to higher climatology SST (Figures S4a–S4c in Supporting Information S1). There is significant negative inter-model correlation between MJO skills and SST thresholds (Figure 3e). A higher inter-model correlation coefficient is found for MJO skills and the difference between SST climatology and threshold (Figure 3f). These results suggest that if the model can trigger the convection more easily over the EWP, it is more likely to exhibit higher MJO simulation skill. Our results are not sensitive to the threshold value of precipitation used (Figure S4 in Supporting Information S1).

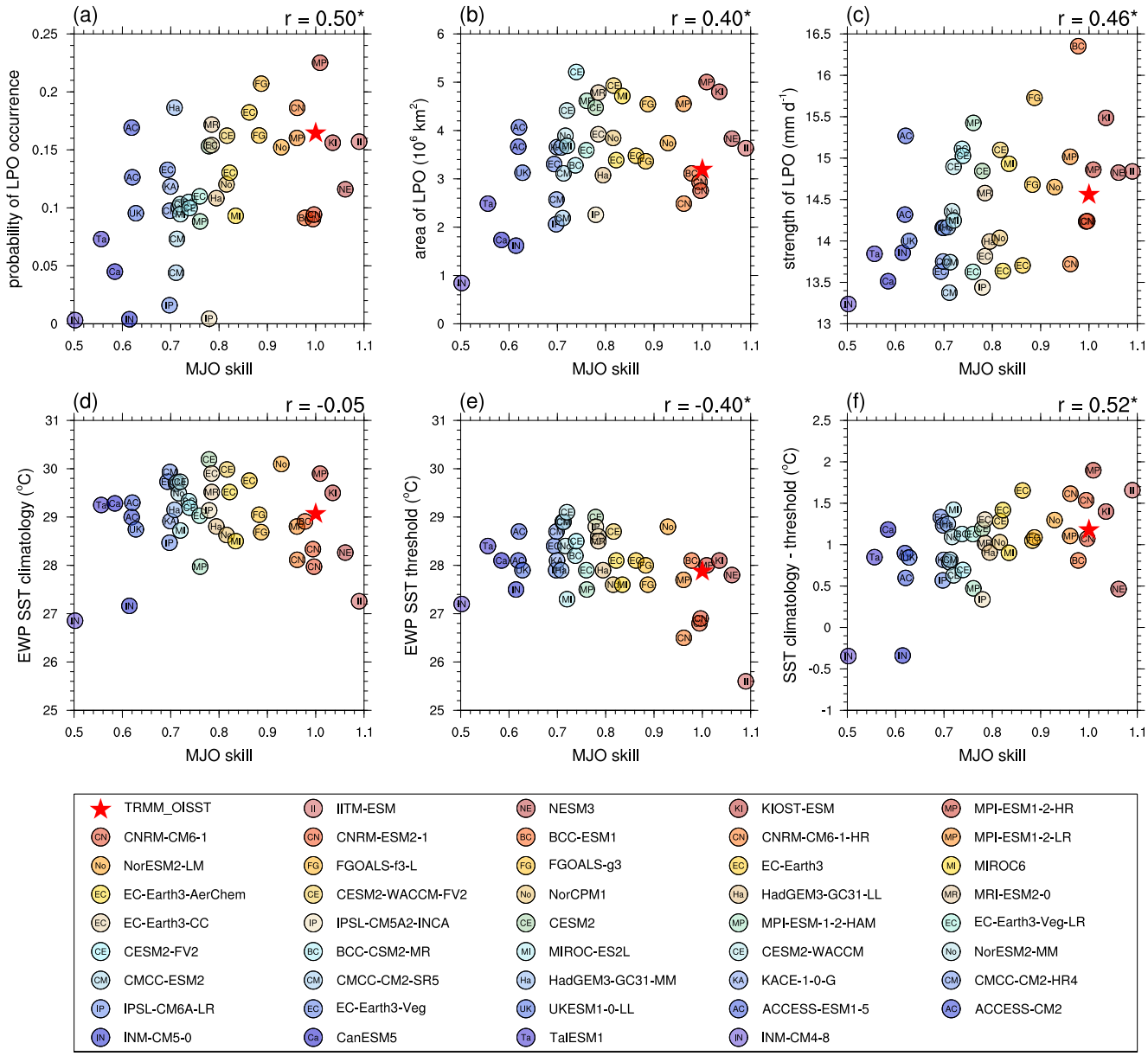

Figure 3. Scatter plots of Madden-Julian Oscillation simulation skills versus (a) the occurrence probability of large-scale precipitation object (LPO), (b) the area (10^6 km^2) of LPO, (c) the strength (mm d^{-1}) of LPO, (d) the sea surface temperature (SST) climatology (°C), (e) the SST threshold for convection (°C), and (f) the differences between the SST climatology and threshold (°C) over the equatorial western Pacific (150°E–180°, 5°S–5°N). Inter-model correlation coefficients are provided in the upper right corner of each panel. Correlation coefficients exceeding 0.3 are treated as significant at the 95% confidence level (marked by asterisk).

The sensitivity of precipitation over the EWP region in response to SST might also be critical to the MJO simulation. Monthly precipitation and SST deviations from the regional mean at each grid over the EWP were used to compute the two-dimensional PDFs of the SST and precipitation (Figures 4a–4d). In the observations, when SST is lower than the regional mean (around 29°C as in Figure 3d), precipitation gradually intensifies as SST increases. When SST exceeds the regional mean, precipitation occurs less frequently (Figure 4a). The top simulations exhibit similar features, but the decrease in precipitation with increasing SST exceeding the regional mean is less than in the observations (Figure 4b). The SST-precipitation relationship in the bottom simulations exhibit different features: The increase in precipitation corresponding to rising SST is slower when the SST is lower, and it continues when SST is high (Figure 4c). Compared to the bottom simulations, the top simulations exhibit stronger precipitation increase when the SST is lower, and their precipitation occurs less frequently when

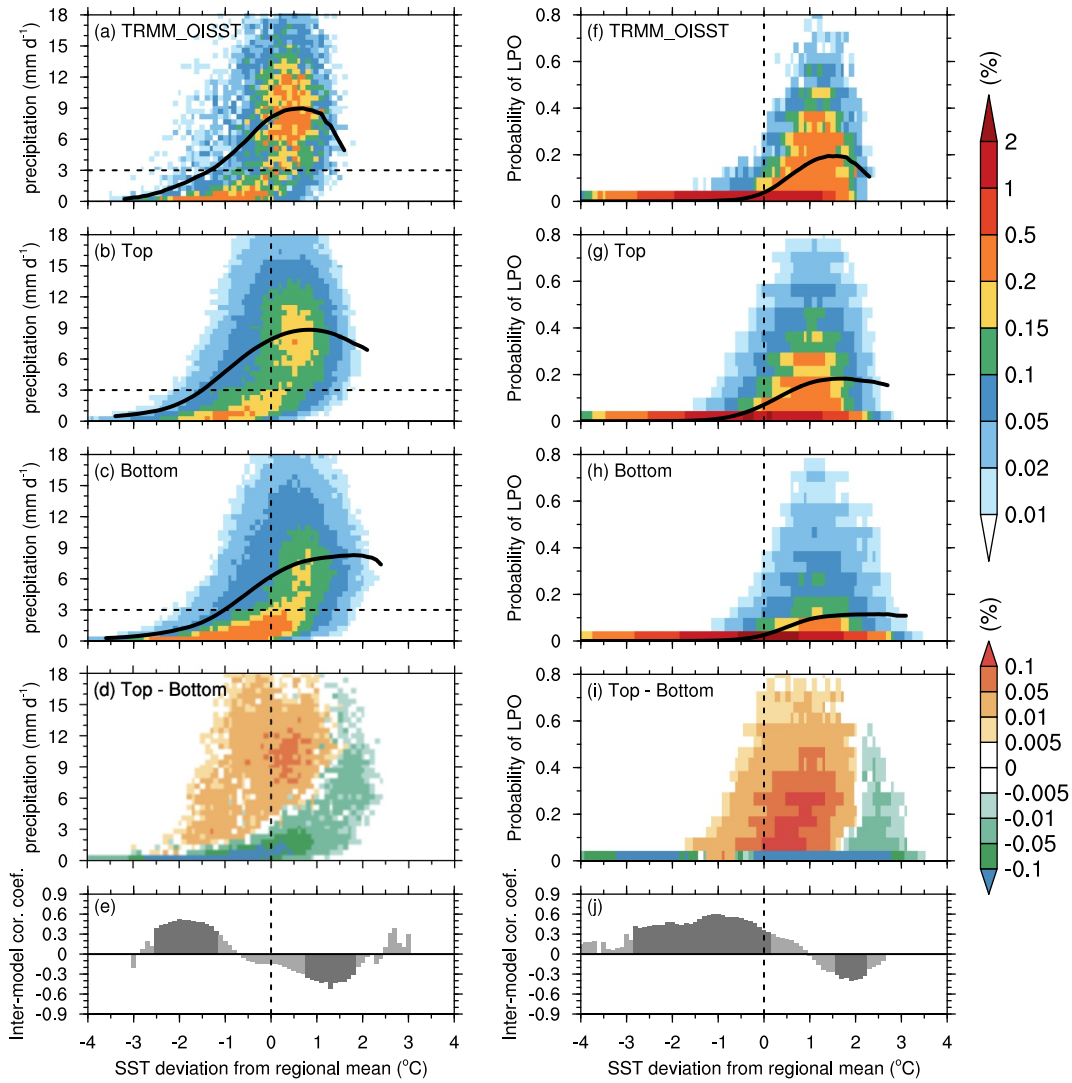

Figure 4. Joint probability distributions (%) of panels (a–d) monthly mean precipitation and (e–h) large-scale precipitation object (LPO) occurrence probability with monthly sea surface temperature (SST) deviations for all the grids from the regional mean over the equatorial western Pacific (150°E–180°, 5°S–5°N) from (a, e) observations, (b, f) the top simulations, (c, g) the bottom simulations, and (d, h) differences between the top and bottom simulations. SST is binned into 0.1°C. Black curves denote the mean values of precipitation and LPO occurrence probabilities as functions of SST bins (sample size of each bin exceeding 0.05% of the total sample size). Panels (e) and (j) show the inter-model correlation coefficients between the slop (11-point fitted) of the black curve of each individual simulations as a function of SST. Black bars indicate that the inter-model correlation coefficients are significant at the 95% confidence level.

the regional SST deviation exceeds 1°C (Figure 4d). Using the raw SST values, similar results can also be obtained but with a wider distribution along *x*-axis (Figure S5 in Supporting Information S1).

The curves in Figures 4a–4c are for averaged precipitation among different SST deviation values with the bin width of 0.1°C for all grids over the EWP. The sensitivity of precipitation to changes in SST can be quantified for each bin using the instantaneous slop of the curves estimated by applying a linear fitting for mean precipitation in 11 centered bins. The inter-model correlation between the sensitivity of precipitation to SST and MJO simulation skills was shown in Figure 4e. The correlation is significant and positive when SST is relatively low and negative when SST is relatively high. If precipitation in a model increases more rapidly with increasing SST when the SST is relatively low, and precipitation decreases more quickly with increasing SST when SST is high, this model tend to exhibit a higher MJO simulation skill. These results suggest if a model cannot reproduce the SST-precipitation relationship realistically over the EWP, it is unlikely to reproduce the MJO well.

The LPO occurrence probability over the EWP is a more direct metric to measure large-scale precipitation organization. The relationship between the monthly mean LPO occurrence probability and SST over the EWP is further compared (Figures 4f–4i). In general, LPO occurs more frequently when SST is higher. The bottom simulations require higher SST to produce the same LPO occurrence probability than in the observations and the top simulations (Figures 4f–4h). Their simulated LPO occurrence probability increases more slowly with increasing SST and tend to continue when SST is high (Figure 4h). These results confirm that accurately simulating the relationship between large-scale precipitation organization and SST is crucial for reproducing the MJO. Similarly, there are also significantly positive (negative) inter-model correlation between MJO skills and the sensitivity of large-scale precipitation organization to SST when the SST is relatively low (high) (Figure 4j). Interestingly, the positive inter-model correlation is higher and spans a wider range in Figure 4j than in Figure 4e. This might imply that the capability of the models to organize large-scale precipitation in relatively lower SST is more critical for MJO simulation.

4. Conclusions and Discussions

In this study, we compared the MJO simulations of 43 CMIP6 models and explored their possible connections to SST-precipitation relationships. Models that exhibit higher MJO simulation skills reproduce more organized large-scale precipitation with spatial scales of thousands of kilometers over the EWP. There is a significant positive inter-model correlation between the MJO simulation skills and the occurrence probability, the spatial scale, and strength of organized large-scale precipitation objects (LPOs) over the EWP. This implies better organization of large-scale precipitation over the EWP in models with higher MJO simulation skills. Previous studies have also revealed the importance of convective organization on an equatorial beta plane to the MJO propagation (Arnold & Randall, 2015; Chen et al., 2021). Tropical convection is organized into different systems such as precipitating cumulus towers, cyclones and convectively coupled waves, spans a wide range of spatiotemporal scales (Kiladis et al., 2009; Mapes, 1993). This study emphasizes the importance of large-scale precipitation organization with spatiotemporal scales of thousands of kilometers and several days to MJO simulations. It is different from the concept of mesoscale organization in terms of spatiotemporal scales, as mesoscale convective systems usually last only for hours (e.g., Houze, 2004, 2018).

A further analysis suggests that more frequent LPOs in the top simulations over the EWP is due to lower SST threshold for convection. Differences between climatology and threshold for convection over the EWP exhibit a higher inter-model correlation with the MJO simulation skills, suggesting that the efficiency of convection trigger over the EWP might be crucial for MJO simulation. The top simulations can reproduce the observed relationship between SST and large-scale precipitation over the EWP more realistically: the large-scale precipitation increases quickly as SST rises, and it is suppressed when the SST is 1–2°C warmer than the climatology. In contrast, in the bottom simulations, the large-scale precipitation increases more slowly as SST rises and remains strong over high SST. These suggests that reproducing the observed relationship between large-scale precipitation and SST over the EWP is critical to MJO simulation.

Models tend to exhibit cold SST biases and underestimate the precipitation over the EWP (Dai, 2006; Li & Xie, 2014). However, the MJO simulation skill is not directly related to the mean SST over the EWP, it is significantly correlated with the meridional and zonal gradients of SST (not shown). This discrepancy implies that the SST gradient over the EWP might be a key factor that modulates the MJO simulation. As SST gradient over the EWP could lead to large-scale convergence, inducing ascending motions and deep convection (Back & Bretherton, 2009; Lindzen & Nigam, 1987). Air-sea interactions, diabatic feedbacks and other factors might also affect the SST-precipitation relationship and MJO simulations (Arnold & Randall, 2015; Liu & Wang, 2013; Martin & Schumacher, 2012; Zhu et al., 2017). Detailed dynamic processes should be further diagnosed.

Improving deep convection parameterizations, such as the entrainment rate, convection trigger, convective adjustment process, and diabatic heating, could improve MJO simulations (Arnold & Randall, 2015; Boyle et al., 2015; Li et al., 2009; Lin et al., 2008; Liu & Wang, 2017; Wang & Schlesinger, 1999; Zhang & Mu, 2005). For example, inclusion of a relative humidity threshold for deep convection trigger improves the MJO simulation (Wang & Schlesinger, 1999; Zhang & Mu, 2005). Organization of large-scale precipitation could be largely determined by the convection trigger function of the deep convection scheme in the models. Further studies based on model sensitivity experiments are needed.

Comparing to the TRMM observations, models generally underestimate the MJO occurrence and amplitude over the Indo-Pacific warm pool by about 50% (Figures S6c–S6d in Supporting Information S1). The inter-model correlation between MJO simulation skills and frequency and amplitude of the MJO peaks over the western Pacific (Figures S6e–S6f in Supporting Information S1). This implies that inter-model differences in their MJO simulations mainly arise from the MJO propagation over the western Pacific. It is consistent with our results that the MJO simulations are most sensitive to large-scale precipitation organization over the EWP. The LPO precipitation can be further categorized into MJO-LPO precipitation and Non-MJO-LPO precipitation (Kerns & Chen, 2020). Both types of LPO precipitation over the EWP exhibits significant inter-model correlations with the MJO simulation skills (Figure S7 in Supporting Information S1), suggesting that inter-model correlation between the MJO simulation skill and the LPO precipitation over the EWP is not determined by the contribution of MJO precipitation to LPO precipitation.

Over the eastern Indian Ocean and Maritime Continent, the MJO simulation skill is not directly associated with the amount of LPO precipitation, it is tightly connected to the portion of MJO-LPO precipitation relative to LPO precipitation (Figure S8 in Supporting Information S1). It implies that reproducing the dynamics that moving the LPO precipitation systems eastward is also important. It requires more efforts in advancing our understanding in the theories and dynamic processes of the MJO over the Indian Ocean and Maritime Continent. For example, the mechanisms of the barrier effect of the Maritime Continent on MJO propagation remain controversial (e.g., Zhang & Ling, 2017), and models generally overestimate such barrier effect (Chen et al., 2020; Ling et al., 2019).

Data Availability Statement

The CMIP6 historical simulation outputs were obtained from https://esgf-node.llnl.gov/search/cmip6/. The TRMM precipitation data set was obtained from the NASA/Goddard Space Flight Center: https://disc.gsfc.nasa.gov/datasets/TRMM_3B42_7/summary. The OISST V2.1 was obtained from NOAA: https://downloads.psl.noaa.gov/Datasets/noaa.oisst.v2.highres/.

Acknowledgments
This research was sponsored by the National Nature Science Foundation of China through Grants 42375065, 42205067 and 41922035. GC acknowledges the support from the Fundamental Research Funds of the Institute of Atmospheric Physics, Chinese Academy of Sciences (E468081801), and the National Key Scientific and Technological Infrastructure project "Earth System Numerical Simulation Facility" (EarthLab; 2023-EL-ZD-00051). PMEL contribution number 5635.

References

Ahn, M. S., Kim, D., Kang, D., Lee, J., Sperber, K. R., Gleckler, P. J., et al. (2020). MJO propagation across the Maritime continent: Are CMIP6 models better than CMIP5 models? *Geophysical Research Letters*, *47*(11), e2020GL087250. https://doi.org/10.1029/2020gl087250

Arnold, N. P., Kuang, Z., & Tziperman, E. (2013). Enhanced MJO-like variability at high SST. *Journal of Climate*, *26*(3), 988–1001. https://doi.org/10.1175/JCLI-D-12-00272.1

Arnold, N. P., & Randall, D. A. (2015). Global-scale convective aggregation: Implications for the Madden-Julian Oscillation. *Journal of Advances in Modeling Earth Systems*, *7*(4), 1499–1518. https://doi.org/10.1002/2015MS000498

Back, L. E., & Bretherton, C. S. (2009). On the relationship between SST gradients, boundary layer winds, and convergence over the tropical oceans. *Journal of Climate*, *22*(15), 4182–4196. https://doi.org/10.1175/2009JCLI2392.1

Biagioli, G., & Tompkins, A. M. (2023). Measuring convective organization. *Journal of the Atmospheric Sciences*, *80*(12), 2769–2789. https://doi.org/10.1175/JAS-D-23-0103.1

Bjerknes, J. (1966). A possible response of the atmospheric Hadley circulation to equatorial anomalies of ocean temperature. *Tellus*, *18*(4), 820–829. https://doi.org/10.1111/j.2153-3490.1966.tb00303.x

Bjerknes, J. (1969). Atmospheric teleconnections from the equatorial Pacific. *Monthly Weather Review*, *97*(3), 163–172. https://doi.org/10.1175/1520-0493(1969)097<0163:ATFTEP>2.3.CO;2

Boyle, J. S., Klein, S. A., Lucas, D. D., Ma, H.-Y., Tannahill, J., & Xie, S. (2015). The parametric sensitivity of CAM5's MJO. *Journal of Geophysical Research: Atmospheres*, *120*(4), 1424–1444. https://doi.org/10.1002/2014JD022507

Chen, G., Chen, S. S., Ling, J., & Li, C. (2021). Large-scale precipitation systems: Essential elements of the Madden-Julian Oscillation. *Geophysical Research Letters*, *48*(14), e2021GL093184. https://doi.org/10.1029/2021GL093184

Chen, G., Ling, J., Li, C., Zhang, Y., & Zhang, C. (2020). Barrier effect of the Indo-Pacific Maritime continent on MJO propagation in observations and CMIP5 models. *Journal of Climate*, *33*(12), 5173–5193. https://doi.org/10.1175/jcli-d-19-0771.1

Chen, G., Ling, J., Zhang, R., Xiao, Z., & Li, C. (2022). The MJO from CMIP5 to CMIP6: Perspectives from tracking MJO precipitation. *Geophysical Research Letters*, *49*(1), e2021GL095241. https://doi.org/10.1029/2021GL095241

Chen, G., Ling, J., Zhang, Y., Wang, X., & Li, C. (2022). MJO propagation over the Indian Ocean and western Pacific in CMIP5 models: Roles of background states. *Journal of Climate*, *35*(3), 955–973. https://doi.org/10.1175/JCLI-D-21-0255.1

Dai, A. (2006). Precipitation characteristics in eighteen coupled climate models. *Journal of Climate*, *19*(18), 4605–4630. https://doi.org/10.1175/JCLI3884.1

Gadgil, S., Joseph, P. V., & Joshi, N. V. (1984). Ocean-atmosphere coupling over monsoon regions. *Nature*, *312*(5990), 141–143. https://doi.org/10.1038/312141a0

Gonzalez, A. O., & Jiang, X. (2017). Winter mean lower tropospheric moisture over the Maritime Continent as a climate model diagnostic metric for the propagation of the Madden-Julian oscillation. *Geophysical Research Letters*, *44*(5), 2588–2596. https://doi.org/10.1002/2016gl072430

Graham, N. E., & Barnett, T. P. (1987). Sea surface temperature, surface wind divergence, and convection over tropical oceans. *Science*, *238*(4827), 657–659. https://doi.org/10.1126/science.238.4827.657

Houze, R. A. (2004). Mesoscale convective systems. *Reviews of Geophysics*, *42*(4), RG4003. https://doi.org/10.1029/2004rg000150

Houze, R. A. (2018). 100 years of research on mesoscale convective systems. *Meteorological Monographs*, *59*, 17.1–17.54. https://doi.org/10.1175/AMSMONOGRAPHS-D-18-0001.1

Hu, S., Xie, S. P., Seager, R., & Cane, M. A. (2023). Spatial and seasonal variations of sea surface temperature threshold for tropical convection. *Journal of Climate*, *36*(15), 4899–4912. https://doi.org/10.1175/JCLI-D-22-0545.1

Huang, B., Liu, C., Banzon, V., Freeman, E., Graham, G., Hankins, B., et al. (2021). Improvements of the daily optimum interpolation sea surface temperature (DOISST) version 2.1. *Journal of Climate*, *34*(8), 2923–2939. https://doi.org/10.1175/JCLI-D-20-0166.1

Huffman, G. J., Bolvin, D. T., Nelkin, E. J., Wolff, D. B., Adler, R. F., Gu, G., et al. (2007). The TRMM multisatellite precipitation analysis (TMPA): Quasi-global, multiyear, combined-sensor precipitation estimates at fine scales. *Journal of Hydrometeorology*, *8*(1), 38–55. https://doi.org/10.1175/jhm560.1

Hung, M. P., Lin, J. L., Wang, W., Kim, D., Shinoda, T., & Weaver, S. J. (2013). MJO and convectively coupled equatorial waves simulated by CMIP5 climate models. *Journal of Climate*, *26*(17), 6185–6214. https://doi.org/10.1175/jcli-d-12-00541.1

Inness, P. M., Slingo, J. M., Guilyardi, E., & Cole, J. (2003). Simulation of the Madden–Julian oscillation in a coupled general circulation model. Part II: The role of the basic state. *Journal of Climate*, *16*(3), 365–382. https://doi.org/10.1175/1520-0442(2003)016<0365:sotmjo>2.0.co;2

Jiang, X., Waliser, D. E., Xavier, P. K., Petch, J., Klingaman, N. P., Woolnough, S. J., et al. (2015). Vertical structure and physical processes of the Madden-Julian oscillation: Exploring key model physics in climate simulations. *Journal of Geophysical Research: Atmospheres*, *120*(10), 4718–4748. https://doi.org/10.1002/2014jd022375

Johnson, N. C., & Xie, S. P. (2010). Changes in the sea surface temperature threshold for tropical convection. *Nature Geoscience*, *3*(12), 842–845. https://doi.org/10.1038/ngeo1008

Kerns, B. W., & Chen, S. S. (2020). A 20-year climatology of madden-Julian oscillation convection: Large-scale precipitation tracking from TRMM-GPM rainfall. *Journal of Geophysical Research*, *126*(7), e2019JD032142. https://doi.org/10.1029/2019jd032142

Kiladis, G. N., Wheeler, M. C., Haertel, P. T., Straub, K. H., & Roundy, P. E. (2009). Convectively coupled equatorial waves. *Reviews of Geophysics*, *47*(2), RG2003. https://doi.org/10.1029/2008RG000266

Lau, K. M., Wu, H. T., & Bony, S. (1997). The role of large-scale atmospheric circulation in the relationship between tropical convection and sea surface temperature. *Journal of Climate*, *10*(3), 381–392. https://doi.org/10.1175/1520-0442(1997)010<0381:TROLSA>2.0.CO;2

Leung, J. C. H., Zhang, B., Gan, Q., Wang, L., Qian, W., & Hu, Z. Z. (2022). Differential expansion speeds of Indo-Pacific warm pool and deep convection favoring pool under greenhouse warming. *npj Climate and Atmospheric Science*, *5*(1), 97. https://doi.org/10.1038/s41612-022-00315-w

Li, C., Jia, X., Ling, J., Zhou, W., & Zhang, C. (2009). Sensitivity of MJO simulations to diabatic heating profiles. *Climate Dynamics*, *32*(2–3), 167–187. https://doi.org/10.1007/s00382-008-0455-x

Li, G., & Xie, S. P. (2014). Tropical biases in CMIP5 multimodel ensemble: The excessive equatorial Pacific cold tongue and double ITCZ problems. *Journal of Climate*, *27*(4), 1765–1780. https://doi.org/10.1175/JCLI-D-13-00337.1

Lin, J., Lee, M., Kim, D., Kang, I., & Frierson, D. M. W. (2008). The impacts of convective parameterization and moisture triggering on AGCM-simulated convectively coupled equatorial waves. *Journal of Climate*, *21*(5), 883–909. https://doi.org/10.1175/2007JCLI1790.1

Lindzen, R. S., & Nigam, S. (1987). On the role of sea surface temperature gradients in forcing low-level winds and convergence in the tropics. *Journal of the Atmospheric Sciences*, *44*(17), 2418–2436. https://doi.org/10.1175/1520-0469(1987)044<2418:OTROSS>2.0.CO;2

Ling, J., Zhang, C., Wang, S., & Li, C. (2017). A new interpretation of the ability of global models to simulate the MJO. *Geophysical Research Letters*, *44*(11), 5798–5806. https://doi.org/10.1002/2017gl073891

Ling, J., Zhao, Y., & Chen, G. (2019). Barrier effect on MJO propagation by the Maritime continent in the MJOTF/GASS models. *Journal of Climate*, *32*(17), 5529–5547. https://doi.org/10.1175/jcli-d-18-0870.1

Liu, F., & Wang, B. (2013). An air–sea coupled skeleton model for the Madden–Julian Oscillation. *Journal of the Atmospheric Sciences*, *70*(10), 3147–3156. https://doi.org/10.1175/JAS-D-12-0348.1

Liu, F., & Wang, B. (2017). Roles of the moisture and wave feedbacks in shaping the Madden–Julian Oscillation. *Journal of Climate*, *30*(24), 10275–10291. https://doi.org/10.1175/JCLI-D-17-0003.1

Madden, R. A., & Julian, P. R. (1971). Detection of a 40–50 day oscillation in the zonal wind in the tropical Pacific. *Journal of the Atmospheric Sciences*, *28*(5), 702–708. https://doi.org/10.1175/1520-0469(1971)028<0702:doadoi>2.0.co;2

Madden, R. A., & Julian, P. R. (1972). Description of global-scale circulation cells in the tropics with a 40–50 day period. *Journal of the Atmospheric Sciences*, *29*(6), 1109–1123. https://doi.org/10.1175/1520-0469(1972)029<1109:dogscc>2.0.co;2

Mapes, B. E. (1993). Gregarious tropical convection. *Journal of the Atmospheric Sciences*, *50*(13), 2026–2037. https://doi.org/10.1175/1520-0469(1993)050<2026:GTC>2.0.CO;2

Martin, E. R., & Schumacher, C. (2012). The relationship between tropical warm pool precipitation, sea surface temperature, and large-scale vertical motion in IPCC AR4 models. *Journal of the Atmospheric Sciences*, *69*(1), 185–194. https://doi.org/10.1175/JAS-D-11-0104.1

Sabin, T. P., Babu, C. A., & Joseph, P. V. (2013). SST–convection relation over tropical oceans. *International Journal of Climatology*, *33*(6), 1424–1435. https://doi.org/10.1002/joc.3522

Sperber, K. R. (2004). Madden–Julian variability in NCAR CAM2.0 and CCSM2.0. *Climate Dynamics*, *23*(3–4), 259–278. https://doi.org/10.1007/s00382-004-0447-4

Waliser, D. E., Graham, N. E., & Gautier, C. (1993). Comparison of the highly reflective cloud and outgoing longwave radiation datasets for use in estimating tropical deep convection. *Journal of Climate*, *6*(2), 331–353. https://doi.org/10.1175/1520-0442(1993)006<0331:COTHRC>2.0.CO;2

Wang, W., & Schlesinger, M. E. (1999). The dependence on convection parameterization of the tropical intraseasonal oscillation simulated by the UIUC 11-layer atmospheric GCM. *Journal of Climate*, *12*(5), 1423–1457. https://doi.org/10.1175/1520-0442(1999)012<1423:TDOCPO>2.0.CO;2

Zhang, C. (1993). Large-scale variability of atmospheric deep convection in relation to sea surface temperature in the tropics. *Journal of Climate*, *6*(10), 1898–1913. https://doi.org/10.1175/1520-0442(1993)006,1898:LSVOAD.2.0.CO;2

Zhang, C., & Ling, J. (2017). Barrier effect of the Indo-Pacific Maritime continent on the MJO: Perspectives from tracking MJO precipitation. *Journal of Climate*, *30*(9), 3439–3459. https://doi.org/10.1175/jcli-d-16-0614.1

Zhang, G. J., & Mu, M. (2005). Simulation of the Madden–Julian Oscillation in the NCAR CCM3 using a revised Zhang–McFarlane convection parameterization scheme. *Journal of Climate*, *18*(19), 4046–4064. https://doi.org/10.1175/JCLI3508.1

Zhu, J., Wang, W., & Kumar, A. (2017). Simulations of MJO propagation across the Maritime continent: Impacts of SST feedback. *Journal of Climate*, *30*(5), 1689–1704. https://doi.org/10.1175/JCLI-D-16-0367.1